Microchimica Acta (2021) 188:228
https://doi.org/10.1007/s00604-021-04877-z

ORIGINAL PAPER

Ethylenediamine-bound magnetite nanoparticles as dual function colorimetric sensor having charge transfer and nanozyme activity for TNT and tetryl detection

Batuhan Yardımcı[1,2] · Ömer Kaan Koç[1,3] · Ayşem Üzer[3] · Jülide Hızal[4] · Reşat Apak[3,5]

Received: 19 February 2021 / Accepted: 25 May 2021

Abstract

A reusable, low–cost, and convenient ethylenediamine (EDA)–bound magnetite nanoparticles (MNPs)–based colorimetric sensor has been developed for dual function colorimetric determination of nitroaromatic explosives such as TNT and tetryl. Colorimetric detection of analytes may occur through two independent routes: (1) nano–Fe_3O_4– EDA– NH_2 as σ–donor may interact with the σ– and π–acceptor aromatic–poly(NO_2) groups to produce a colored charge–transfer (CT) complex; (2) nano –Fe_3O_4–EDA–NH_2 as a Fenton-type nanozyme may generate reactive species that comprise hydroxyl radicals ($^{\bullet}OH$) with H_2O_2 to oxidize 3,3′,5,5′–tetramethylbenzidine (TMB) to a blue-colored diimine (oxTMB–TMB) CT complex, where this color is bleached with TNT/tetryl because of donor–acceptor interactions between the explosive –NO_2 groups and the –NH_2 group of Fe_3O_4–EDA nanoparticles of restricted nanozyme activity. Both methods can quantify TNT well below the EPA recommended TNT residential screening level in soil, LOD being in the micromolar range. As EDA was covalently bound to MNPs, the same sensor can be separately reused six times for TNT and eight times for tetryl determination, using method (1). Common metal ions, anions, energetic materials, several camouflage materials, and soil components such as humates did not interfere with the nanosensor performance for TNT and tetryl. The combination of charge–transfer and nanozyme ability of Fe_3O_4– EDA –NH_2 nanoparticles may bring a new approach to dual function colorimetric sensor design. To the best of our knowledge, this is the first dual function colorimetric sensor for TNT and tetryl using the same nanoparticles as sensing elements in two different detection systems involving either formation or bleaching of colored species.

Keywords Dual function colorimetric sensor · Nitroaromatic explosives · Charge–transfer complex · Spectrophotometric determination · Amine functionalized nanoparticles

Introduction

2,4,6–Trinitrotoluene (TNT) is a nitroaromatic explosive that was widely released into soil and water ecosystems after intensive use during both world wars (without mentioning post-war activities). Therefore, many sites used for the production of TNT are severely contaminated with explosives and related compounds [1,2]. Typical areas may be contaminated with TNT up to 10 g kg^{-1} in soils and up to 100 mg L^{-1} in water samples. Tetryl is also responsible for environmental pollution in soil and groundwater [3]. Tetryl is also toxic and mutagenic to several different bacteria. Dermatitis has also been observed after prolonged exposure to this explosive substance [4]. In this context, numerous analytical methods have been developed to measure traces of TNT and tetryl in complex environmental matrices. Due to the electron withdrawing nitro groups attached to the aromatic ring, these substances can interact

✉ Reşat Apak
rapak@istanbul.edu.tr

1 Institute of Graduate Studies, Chemistry Department, Istanbul University-Cerrahpaşa, Avcilar, Istanbul, Turkey

2 Science and Technology Application and Research Center (ARTMER), Zonguldak Bulent Ecevit University, Kozlu, Zonguldak, Turkey

3 Engineering Faculty, Chemistry Department, Istanbul University-Cerrahpaşa, Avcilar, Istanbul, Turkey

4 Engineering Faculty, Chemical and Process Engineering Department, Yalova University, Yalova, Turkey

5 Turkish Academy of Sciences (TUBA), Cankaya, Ankara, Turkey

Published online: 11 June 2021

with other electron–rich donor molecules as proton donors, σ– and π– acceptors, H−bond acceptors, and electron–transfer agents via π stacking feature, forming the basis of various spectroscopic techniques used in their determination [5].

Many spectroscopic methods have been applied to the detection of TNT and/or tetryl such as colorimetry [6,7], terahertz spectroscopy [8], photo–thermal infrared imaging spetroscopy [9], ion mobility spectrometry [10], mass spectrometry [11], and infrared and Raman spectroscopy [12]. The presence of electroactive nitro groups also gave way to electrochemical detection techniques [13,14].

Miniaturization and portability are required to develop and improve analytical techniques. Nanoparticle–based colorimetric sensors have some advantages, such as small size and large specific surface area, enhanced reactivity, high sensitivity, and embedding ability into thin films and other matrices that can be attached to paper and optical devices suitable for automatic analysis. Nanotechnology and nanostructured materials are finding increased use in science and technology, and as a part of these nanomaterials, MNPs are on the rise for applied research fields such as analytical chemistry, biosensing, and nanomedicine [15]. The combination of magnetically separable nanoparticles with various analytical methods has enabled operations such as sensing [16,17], capture of analyte [18], and wastewater purification [19]. Many synthesis methods of magnetic nanoparticles were developed with different functional groups linked to their surfaces [15,20].

3,3′,5,5′–Tetramethylbenzidine (TMB) is a safe (non–mutagenic) chromogenic reagent and a horseradish peroxidase (HRP) substrate that can form a charge transfer (CT) complex with its oxidized form [21] to form a blue solution [22]. TMB requires a peroxidase-like catalyst to form this blue CT complex with H_2O_2 acting as oxidant. Magnetite (Fe_3O_4) nanoparticles acting as nanozymes have been first discovered in 2007 to display intrinsic peroxidase–like behavior, with HRP–like catalytic activity [23]. Fe_3O_4 NPs (MNPs) were shown by our research group to give a Fenton–like reaction with H_2O_2 to generate hydroxyl radicals ($^{\bullet}OH$) [24] that can oxidize TMB to the blue–colored CT complex showing maximal absorption at the 650–nm wavelength. Nanozymes such as MNPs generally give rise to more robust analytical determinations than peroxidase enzymes due to their lower sensitivity to pH and temperature changes than enzyme proteins [23]. This study aims to demonstrate a similar peroxidase–like behavior of EDA–derivatized MNPs and to exploit this feature in an indirect TNT/tetryl assay.

TNT is known to form a charge transfer complex with various amines, including dicyclohexylamine (DCHA) [7,25], isopropylamine, tetraethylene–pentamine, and bis(3–aminopropyl)amine [26]. Among these, ethylenediamine (EDA) was found to provide the most stable complex with the largest association constant [26]. It is well known that strong acid–base pairing interaction occurs between the electron–rich amino groups and electron–deficient nitroaromatic rings [27–29]. TNT, a typical electron–deficient nitro compound, can selectively interact with primary amines to form TNT−amine complexes through the charge transfer from the donor (amine group) to the acceptor (nitroaromatic group). This specific interaction makes it feasible to design the surface chemistry of nanomaterials for the selective and sensitive detection of TNT [29–31].

In this study, EDA–modified MNPs were synthesized, as described by Songvorawit et al., [32] by necessarily changing some parameters regarding the single step "polyol synthesis" of amino–functionalized MNPs for the manufacture of a sensitive, reusable, and low–cost MNPs–derivatized colorimetric sensor to detect TNT/tetryl. The detection principle is related to CT–complexation between free $–NH_2$ group of EDA–modified MNPs and $–NO_2$ groups of TNT/tetryl, and this active principle is predominant in both procedures (methods −1 and 2) using the developed sensor. Although SERS [33], voltammetric [34], and fluorometric [35] methods have been reported for TNT determination using modified MNPs, this EDA–bound MNPs sensor is the first of its kind in reliably determining TNT/tetryl by giving rise to two distinct colorimetric procedures comprising charge−transfer and redox catalysis. Both procedures proved to be sufficiently sensitive to quantify TNT in synthetically contaminated soil with LOQ below the concentration levels set by US EPA for soil remediation (the residential soil screening level (SSL) of TNT was 21 mg kg^{-1}, while 79 mg kg^{-1} was set for industrial SSL) [36].

Experimental

Materials and chemicals

Ethanol (EtOH), acetone, acetonitrile (AcCN), ethylene glycol ($HOCH_2CH_2OH$), ethylenediamine (EDA), 3,3′,5,5′–tetramethylbenzidine (TMB), and humic acid were purchased from Sigma–Aldrich (St. Louis, MO, USA, www.sigmaaldrich.com). Iron (III) chloride hexahydrate ($FeCl_3.6H_2O$), sodium acetate (CH_3COONa), sodium hydroxide (NaOH), 2,4,6–trinitrophenol (picric acid, PA), and dimethyl sulfoxide (DMSO) were obtained from Merck (Darmstadt, Germany, www.merckmillipore.com). The explosive materials TNT (pure), tetryl (pure), 1,3,5–trinitroperhydro–1,3,5–triazine (RDX, which contains 85% active coumpound), 1,3,5,7–tetranitro–1,3,5,7–tetraazacyclooctane (HMX, pure), composite B (60% RDX + 39% TNT + 1% wax), composite C–4 (91% RDX + 5.3% di(2–ethylhexyl) sebacate +2.1% polyisobutylene +1.6% fuel oil), tetrytol (70% tetryl +30% TNT), octol (70% HMX + 30% TNT), pentaerythritol tetranitrate (PETN, pure), ammonium nitrate (AN), and 2,4–dinitrotoluene (DNT, pure) were kindly supplied by the Mechanical and Chemical Industry Corporation

(Makine Kimya Endustrisi Kurumu, MKEK, www.mkek.gov.tr) of Turkey. 1,3,5–Triamino–2,4,6–trinitrobenzene (TATB) explosive was provided by AccuStandard. RTC blended sandy soil (clean sandy soil), used as a sample for the determination of explosives such as TNT, tetryl, and tetrytol in the soil, was purchased from Sigma-Aldrich.

Instruments

Shimadzu AUX320 brand balance and Wisd brand Vortex device were used for preparation of standard and working solutions; IKA C–MAG magnetic stirrer heater was used for synthesizing EDA–modified MNPs. Wisd WiseBath water bath was used for setting the optimal temperature conditions of the proposed sensor. Shimadzu UV–1800 spectrophotometer and Hellma Suprasil quartz cuvettes (optical thickness 10 mm) were used for all absorption measurements. Ultrapure water used in the analysis was provided from Merck Millipore–Direct–Q® 8 UV Remote Water Purification System (Water resistivity is 18 MΩ·cm). A magnet was used to purify and precipitate EDA–modified MNPs. The proposed method was validated against a gas chromatographic/mass spectrometric (GC–MS) method [37] and a liquid chromatographic/mass spectrometric (LC–MS/MS) method [38] in the literature. A Thermo Scientific Trace gas chromatograph coupled with a DSQII mass spectrometer containing electron impact ionization and a quadrupole analyzer was used. The GC was equipped with a Thermo TR–HT5 column (15 m × 0.25 μm, ID 0.1 μm, 5% phenyl polycarborane siloxane). LC–MS/MS analysis was performed using a Shimadzu 8040 LC–MS liquid chromatography–mass spectrometer equipped with two mass spectrometers containing an electrospray ionization source with a quadrupole mass analyzer. The column was a Restek Ultra AQ C18 (3 μm by 100 × 2.1 mm inner diameter). The infrared spectra were recorded with diffuse reflectance infrared Fourier–transform spectroscopy (DRIFT) using a Bruker–Alpha T model spectrophotometer in the 4000–400 cm^{-1} range.

Preparation of solutions

Detailed information about all solutions prepared in this study takes place in the "Electronic Supplementary Material."

Synthesis, modification, and characterization of ethylenediamine–modified MNPs

MNPs functionalized with EDA were synthesized using the polyol technique as described by Songvorawit et al. [32] with some differences. Details of the synthesis route are presented in "Electronic Supplementary Material."

Recommended procedure for TNT and tetryl determination with methods–1 and 2

For method–1, a volume of 0.5 mL of 1.6% (*w*/*v*) dispersed solution of EDA–modified MNPs in DMSO and 0.5 mL each of TNT solutions in acetone at different initial concentrations (2.0–50.0 mg L^{-1}) were mixed in an Eppendorf tube. For the blank solution, 0.5 mL of 1.6% (*w*/*v*) dispersed solution of EDA–modified MNPs in DMSO was mixed with 0.5 mL of pure acetone. The samples and blank solution in the Eppendorf tubes were kept in a water bath at 55 °C for 10 min. The same procedure was applied for tetryl solutions in acetone at different initial concentrations between 2.0 and 20.0 mg L^{-1}, and then EDA–modified MNPs were precipitated with the aid of a magnet. The absorbance values of supernatants were measured against the blank solution at 512 nm wavelength.

Summarized procedure of method–1, 0.5 mL of 1.6% (*w*/*v*) EDA–modified MNPs+ 0.5 mL TNT/tetryl solution in acetone → keep in water bath at 55 °C for 10 min → ppt. MNPs → measure supernatant abs.: $A_{512\ nm}$ vs. reagent blank.

For method–2, 3.25 mL of 20.0 mg EDA–modified MNPs dispersed in 25.0 mL of ultrapure water were taken and transferred to an empty flask. To the EDA–modified MNPs, 10.0 mL of stock H_2O_2 (1.0×10^{-2} M), 2.5 mL of acetate buffer (1.0 M, pH 4.0), and 5.0 mL of stock TMB solution (1.0×10^{-3} M) prepared in ethanol were added and left in the dark for 60 min to equilibrate. At the end of this period, 0.5 mL of the blue MNPs–TMB solution was added to the Eppendorf tubes. Then, increasing amounts (5.0–80.0 mg L^{-1} for TNT, 10.0–100.0 mg L^{-1} for tetryl) of TNT/tetryl solutions prepared in acetone were added separately to the tubes. Finally, ultrapure water was added to Eppendorf tubes with a volume of 1.0 mL. Tubes containing TNT were kept at room temperature (25 °C) for 5.0 min, tubes containing tetryl for 10.0 min at 25 °C, and UV–Vis spectra of all tubes were taken. The changes (decrements) in the absorbance of solutions at 650 nm wavelength were taken as a measure of inhibition by nitro explosives of the nanozyme activity of EDA–MNPs.

Summarized procedure of method–2, 0.5 mL of MNPs–equilibrated TMB solution+ 0.5 mL TNT/tetryl solution in acetone → keep at room temperature (25 °C) in optimized time (5 and 10 min for TNT and tetryl, respectively) → measure solution absorbance: $A_{650\ nm}$ vs. reagent blank.

Study of synthetic mixtures of TNT and tetryl

Synthetic mixture solutions of TNT and tetryl (in the mass ratio varying between 1:1 to 10:1) were prepared with suitable mixing of 100.0 mg L^{-1} TNT and 50.0 mg L^{-1} tetryl stock solutions, and dilution to yield final mixtures containing 4.0 mg L^{-1} tetryl (in all mixture samples) and increasing

concentrations of TNT. The proposed sensing methods–1 and –2 were applied to these mixture solutions.

Determination of TNT in the presence of common soil ions and energetic materials

Common soil ions (Cl^-, NO_3^-, SO_4^{2-}, K^+, Mg^{2+}, Ca^{2+}, Al^{3+}); most used energetic materials such as RDX, HMX, and tetryl; soil component such as humic acid; and camouflage materials such as sugar, sweetener, acetylsalicylic acid, paracetamol–caffeine–based painkiller, and detergent were separately mixed with a TNT solution at an initial concentration of 20.0 mg L^{-1} with respect to methods–1 and 2. Additionally, solutions were prepared with an initial concentration of 20.0 mg L^{-1} TNT–equivalent in composite B, composite C–4 and octol. The developed sensing procedure was applied to these mixture solutions (of composite explosives) and TNT recovery values were calculated (details given in "Electronic Supplementary Material").

Application of the proposed sensor to real soil samples

A weight of 2.0 g sandy soil each was transferred to a series of beakers and 2.5 mL of 100.0 mg L^{-1} TNT, 80.0 mg L^{-1} tetryl, and tetrytol (60.0 mg L^{-1} TNT + 140.0 mg L^{-1} tetryl) solutions in acetone were separately used to contaminate these soils. Synthetically contaminated soil samples were homogenized using ultrasonic bath and then dried at 50 °C. Extraction process was applied to each contaminated soil sample with the final volume of 25.0 mL in acetone and then filtered (CHROMAFIL, PET–20/25). The sensing methods–1 and 2 were applied to the soil extracts diluted 10 times for analysis.

Method validation of the developed sensor against GC–MS and LC–MS/MS using TNT and tetryl samples

For validating methods–1 and 2, the reference GC–MS and LC–MS/MS method was used as described in the literature [37,38]. Application of GC–MS and LC–MS/MS method to the analytes (TNT and tetryl) and appropriate conditions were described in "Electronic Supplementary Material."

Results and discussion

Optimization of the sensor parameters

Some critical parameters for selecting the optimal conditions of the proposed sensing methods, such as suitable volume of EDA for functionalizing MNPs, time, and temperature, were described in "Electronic Supplementary Material."

Synthesis, modification, and characterization of ethylenediamine–modified MNPs

The EDA–modified MNPs were synthesized based on the procedure described in literature. The important advantages of the procedure were single step synthesis and long–term stability of the synthesized MNPs; EDA can be effectively functionalized on the surface of nanoparticles without requiring a second modification step (Scheme 1).

Infrared spectrum (obtained with KBr powder) was taken and SEM images were recorded at different zoom levels for the structural characterization of the synthesized nanoparticles. When the infrared spectrum shown in Fig. 1a is examined, the Fe–O stretching band of the MNPs (Fe_3O_4) is seen at around 642 cm^{-1}. The two peaks around 2939 and 2879 cm^{-1} belong to the C–H vibration of the $–CH_2$ group, and the single peak around 957 cm^{-1} to the C–H stretching band. The $–CH_2$ scissoring band is seen at 1527 cm^{-1}. Although the N–H stretch band is observed at around 1670 cm^{-1}, the characteristic N–H vibration giving rise to two bands of $–NH_2$ are observed at 3520 and 3443 cm^{-1}.

In the characterization phase, SEM images of EDA–modified MNPs at different zoom levels were recorded. According to SEM results, size distribution of EDA–modified MNPs were approximately between 57 and 70 nm (Fig. 1b).

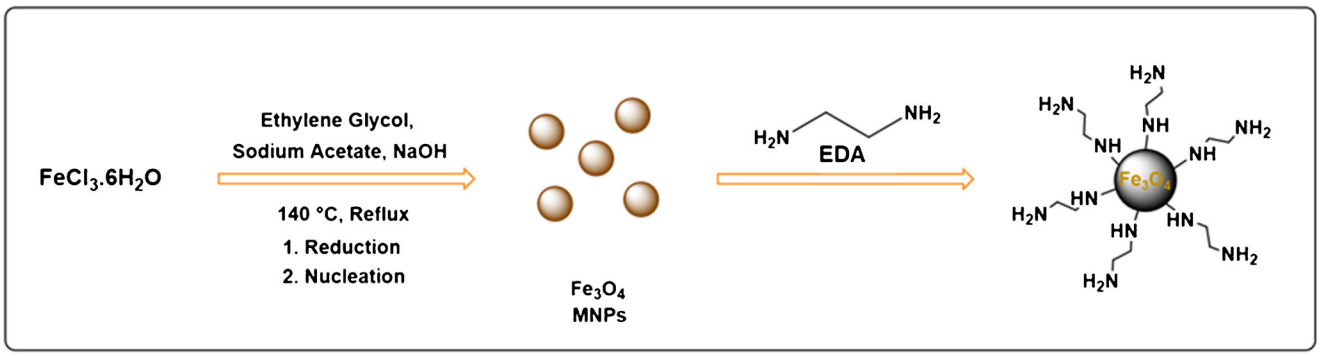

Scheme 1 Schematic illustration of the synthesis process for EDA–modified magnetite nanoparticles (MNPs)

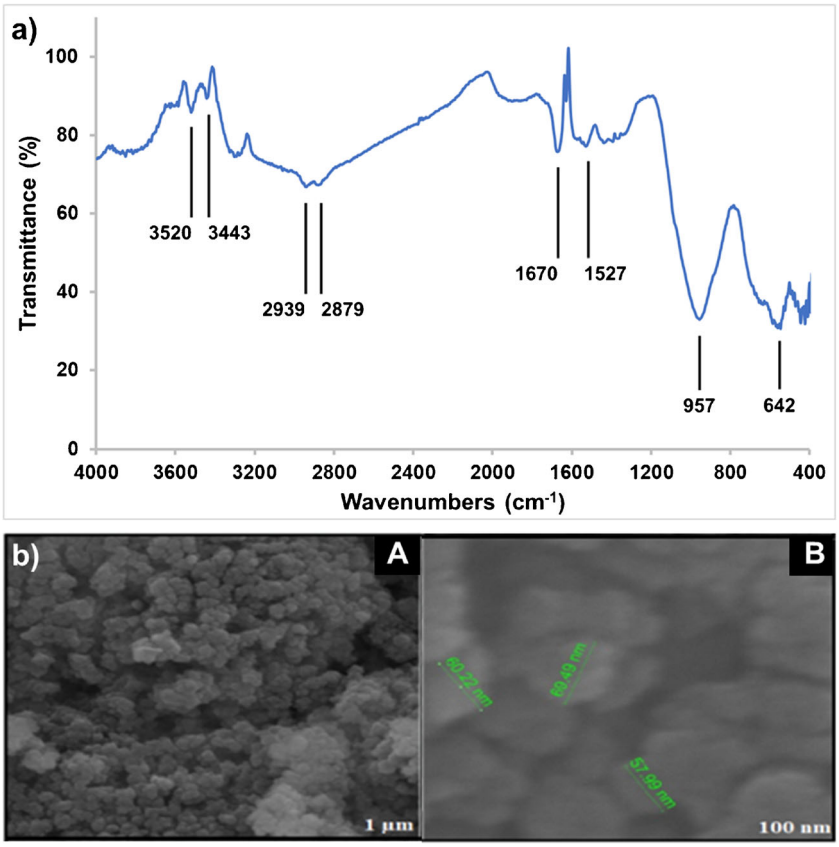

Fig. 1 **a** Infrared (using KBr powder) spectra of EDA–modified MNPs. **b** SEM images at 1 µm (A, 100000×), representation of nanoscale at 100 nm (B, 800000×)

Working principle of the sensor

The covalent functionalization of MNPs with EDA is shown in Scheme 1. This was necessary to firmly attach EDA to the MNPs surface, as both methods−1 and 2 made use of the $–NH_2$ functional groups of modified nanoparticles which would not detach upon sensing reactions as required for repeated use of the sensor. The developed sensor can detect nitroaromatic explosives with two different methods. It has been established that Meisenheimer complexes form between an electron–deficient nitroaromatic compound and an electron–rich amine [39]. Three and four nitro groups in TNT and tetryl, respectively, attract electrons from a charge–donating primary amine EDA located on MNPs to form Meisenheimer complexes. This Meisenheimer complex allows a colorimetric detection of TNT and tetryl in the UV–visible region. Thus, method−1 for TNT and tetryl sensing with EDA–MNPs relies on this donor−acceptor complexation (Scheme 2a).

In method–2, the sensor is not directly activated with TNT and tetryl. Firstly, the peroxidase–mimic EDA–MNPs having nanozyme activity react with hydrogen peroxide (H_2O_2) to generate reactive species that can oxidize the peroxidase substrate TMB to a blue–colored product in acetate buffer (at pH 4.0). The blue color of oxidized TMB arises from its capability of forming a CT–complex with unoxidized TMB. TNT and tetryl compounds added to the medium interact with EDA–MNPs to partially inhibit their nanozyme activity, reverse the CT–complex formation of TMB, and cause a bleaching of the blue color by disrupting the charge–transfer complex formed from TMB, and thus colorimetric determination of these molecules is made possible by this absorbance decrement at 650 nm (Scheme 2b).

In order to better understand the interaction between EDA–modified MNPs and TNT (or tetryl) in method–2, the procedure was repeated with EDA–unmodified MNPs (or bare MNPs). At the end of the experiment, blue color formation was observed in the solution containing TNT, like in the solution without TNT. This shows that TNT cannot interact with bare MNPs not functionalized with the $–NH_2$ group of EDA, and as a result, the Fenton reaction of bare MNPs with H_2O_2 giving rise to TMB coloration cannot be prevented.

Analytical performance of the proposed sensor applied to TNT and tetryl samples

"Optimization of reaction conditions and proposed sensing parameters," "selection of optimal time for sensing procedure," "selection of optimal temperature for sensing procedure," "selection of optimal interaction time for MNPs with TMB," "selection of optimal interaction time for TNT and tetryl with MNPs–TMB," "Investigation of the sensor activity

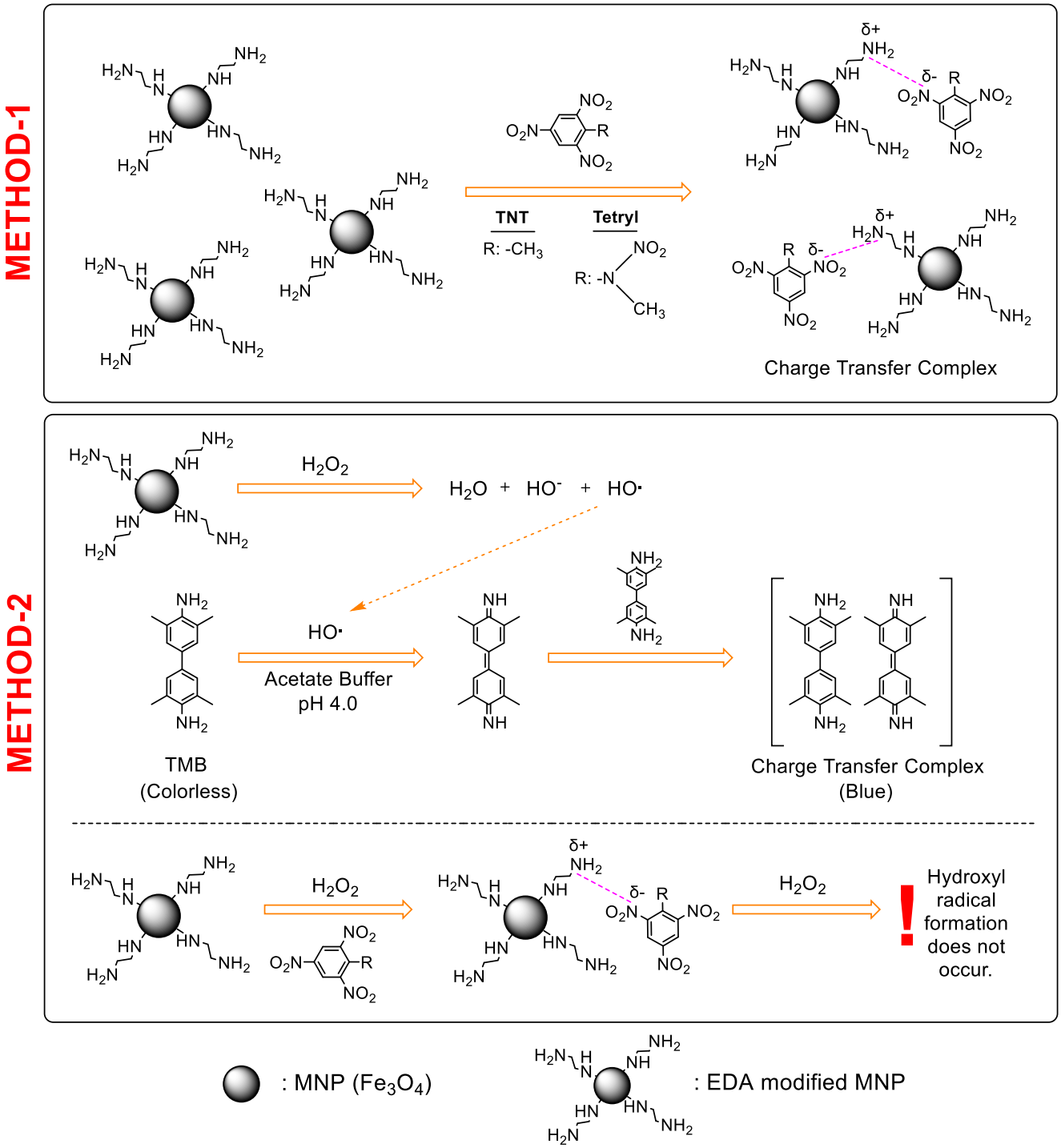

Scheme 2 **a** Method–1 and **b** method–2 interaction scheme of EDA–modified MNPs for TNT and tetryl determination

depending on the pH change in the application of method–2," and "Calibration plots obtained for TNT and tetryl samples by application of method–1 and method–2" parts are presented in "Electronic Supplementary Material." The figures for the relevant sections are presented as Figs. S1, S2, S3, S4, S5, S6, S7, and S8.

The developed sensing (methods–1 and 2) procedures were applied to different concentrations of TNT/tetryl solutions. In method–1, as the concentration of TNT/tetryl solutions increased, the color of TNT solutions changed from pink to purple, and the color of tetryl solutions changed from light pink to dark pink. All absorbance measurements were made against a blank solution at 512 nm wavelength. The blank solution was prepared as described in the sensing method–1, where dispersed solution of EDA–modified MNPs in DMSO was mixed with pure acetone. In method–2, increasing

concentrations of TNT/tetryl solutions were added to the previously prepared MNPs–TMB solution to monitor the color changes. It was observed that the blue color of the MNPs–TMB solution with increasing TNT/tetryl concentration became light blue by bleaching.

The absorbance changes of all prepared solutions were examined at 650 nm wavelength. All measurements were made against water. The calibration equations for determining TNT (Eqs. 1a and 1b) and tetryl (Eqs. 2a and 2b) were generated from the absorbance values at 512 nm for method–1 and at 650 nm for method–2.

Linear calibration equations for TNT:

$$A_{512} = (7.17 \pm 0.10) \times 10^3\, C_{TNT} + (4.47 \pm 0.63) \times 10^{-2}\ (N = 7, r = 0.9995) \quad (1a)$$

$$\Delta A_{650} = (1.70 \pm 0.0088) \times 10^3\, C_{TNT} - (1.20 \pm 0.0042) \times 10^{-3}\ (N = 9, r = 0.9980) \quad (1b)$$

where C_{TNT} is the TNT concentration (in mol L^{-1}) in final solution.

Linear calibration equations for tetryl:

$$A_{512} = (2.06 \pm 0.04) \times 10^4\, C_{tetryl} + (2.84 \pm 0.80) \times 10^{-2}\ (N = 5, r = 0.9995) \quad (2a)$$

$$\Delta A_{650} = (8.90 \pm 0.0026) \times 10^3\, C_{tetryl} + (9.00 \pm 0.0016) \times 10^{-4}\ (N = 10, r = 0.9978) \quad (2b)$$

where C_{tetryl} is the tetryl concentration (in mol L^{-1}) in final solution.

Visible spectra of EDA–modified MNPs for different concentrations of TNT with the color changing from pink to purple (method–1), from blue to light blue (method–2) and for different concentrations of tetryl, color changing from light pink to dark pink (method–1), from blue to light blue (method–2) are shown in Fig. 2 and Fig. 3, respectively.

The validation parameters for the analytical performance of the developed sensor for TNT and tetryl determination are summarized in Table 1. The limit of quantification (LOQ) was well below the EPA recommended TNT residential screening level in soil (21 mg kg^{-1} or 21 ppm) [36].

In addition, a comparison between these methods and other methods published in the literature for TNT and tetryl determination with respect to the linear ranges and detection limits was given in Table S3, together with a relevant comment for table data in the Supplementary Material.

Investigation of selectivity of the sensor

The sensor developed in both methods responded to both TNT and tetryl. To observe the responses of other nitro explosives to the sensor for selectivity testing, explosives (DNT, PA, HMX, RDX, PETN, AN, TATB) at a final concentration of 500.0 mg L^{-1} were interacted with EDA–MNPs in solution. The reason for choosing these compounds was their possibility of formation of CT–complexes with the derivatized MNPs.

Either color formation (method−1) or color bleaching (method−2) was not observed at high concentrations when the developed sensing procedure was applied to DNT, PA, HMX, RDX, PETN, AN, and TATB (Fig. 4). Picric acid did not interact with the $–NH_2$ group of EDA–modified MNPs due to its intrinsic intramolecular CT.

In addition, it was investigated whether DMSO (i.e., a Lewis basic solvent) alone can give a CT–complex with 500.0 mg L^{-1} (final conc.) TNT or tetryl when the developed sensor method–1 procedure was applied without using EDA–

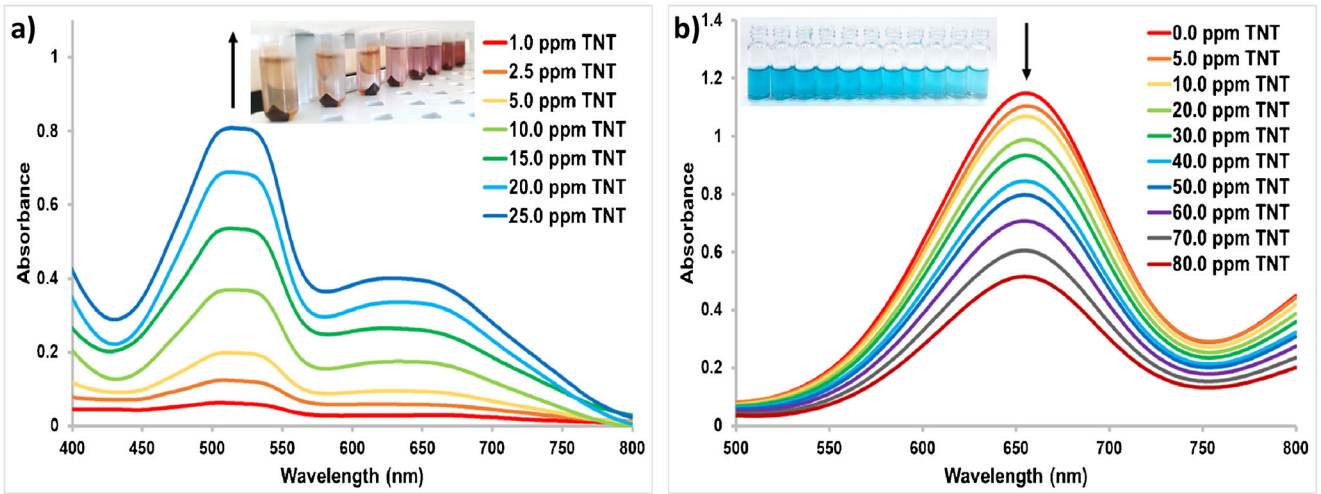

Fig. 2 Visible spectra of **a** the supernatants of EDA–modified MNPs mixed with different concentrations of TNT in pure acetone (method–1) (inset: photograph of the supernatants of EDA–modified MNPs mixed with different concentrations of TNT in pure acetone), **b** the EDA–modified MNPs–TMB solutions containing different concentrations of TNT in aqueous medium (method–2) (inset: photograph of the EDA–modified MNPs mixed with different concentrations of TNT in pure acetone)

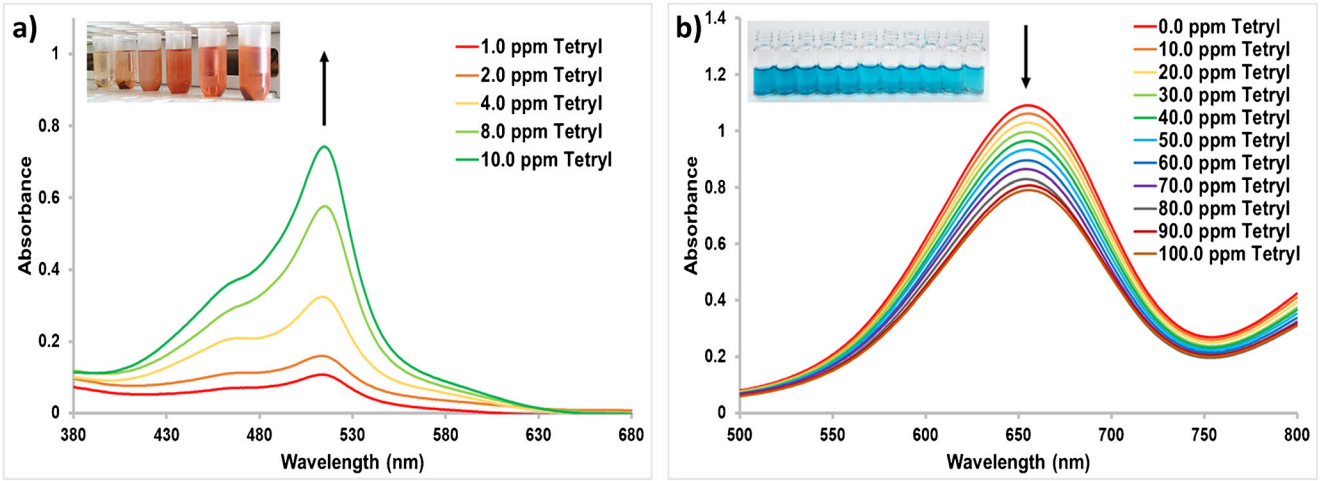

Fig. 3 Visible spectra of **a** the supernatants of EDA–modified MNPs mixed with different concentrations of tetryl in pure acetone (method–1) (inset: photograph of the supernatants of EDA–modified MNPs mixed with different concentrations of tetryl in pure acetone), **b** the EDA–modified MNPs–TMB solutions containing different concentrations of tetryl in aqueous medium (method–2) (inset: photograph of the EDA–modified MNPs mixed with different concentrations of tetryl in pure acetone)

MNPs. No color formation was observed in DMSO mixture solutions with TNT or tetryl.

Evaluation of reusability of the developed sensor for TNT/tetryl determination

Solutions of TNT at an initial concentration of 20.0 mg L^{-1} and tetryl at 8.0 mg L^{-1} in acetone were prepared for testing the reusability of the proposed sensor in method–1. Firstly, the recommended procedure was applied to the determination of TNT at 20.0 mg L^{-1}. The EDA-modified MNPs were precipitated with a magnet and the absorbance of the supernatants was measured against that of the blank solution at 512 nm wavelength. Secondly, after removal of the supernatant of precipitated EDA–MNPs in Eppendorf tubes, 0.5 mL DMSO and 0.5 mL of 20.0 mg L^{-1} TNT were added and vortexed. The sensing (applied to TNT and tetryl solutions), magnetic precipitation, and $A_{512\ nm}$ measurement procedures were repeated over and over for EDA–MNPs until a minimal absorbance value of 0.1 was reached. As Zhu et al. pointed out, magnetic separation significantly reduced scattering noise and background signal, and was useful for improving sensitivity [40]. It was concluded that the EDA–modified MNPs can be used successively six times to detect TNT (Fig. S9) and eight times to detect tetryl (Fig. S10) without loss of accuracy in determination. It should further be noted that the sensing nanoparticles can be equally effective even when the adsorbed trace TNT (in the form of surface CT–complex) was not washed with acetone each time before reuse of EDA–MNPs. Three replicates were studied for three separate samples during each day to generate relevant graphs.

Evaluation of TNT recovery in complex matrices

In both methods using the developed sensor, TNT and tetryl were determined at the same wavelength of the adopted

Table 1 Analytical performance parameters of the developed sensor for TNT and tetryl

Analyte	Method	Linear range[a]	LOD[b]	CV[c] (%)	
				Intra-assay	Inter-assay
TNT	1	4.40×10^{-6} – 1.10×10^{-4}	0.25	0.43	0.78
	2	2.20×10^{-5} – 3.52×10^{-4}	0.95	0.54	0.68
Tetryl	1	3.48×10^{-6} – 3.48×10^{-5}	0.10	0.64	0.69
	2	4.40×10^{-6} – 1.10×10^{-4}	1.75	0.71	0.61

[a] In molar units at final concentration

[b] Limit of detection, in milligrams per liter units (LOD = 3 σ_{bl}/m, σ_{bl} denoting the standard deviation of a blank and m showing the slope of the calibration line)

[c] Coefficients of variation, as percentage ($N = 5$)

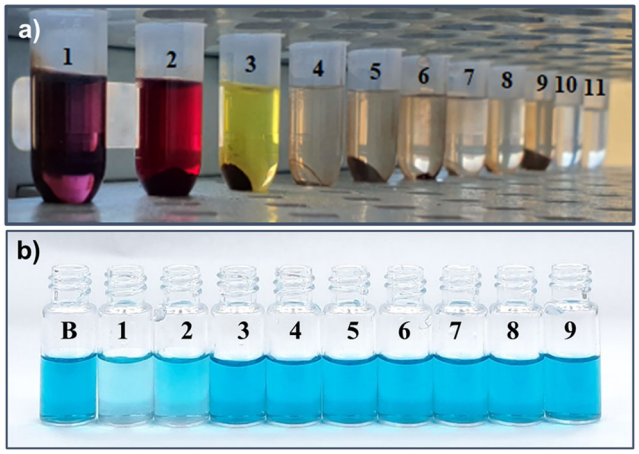

Fig. 4 Color formation with the proposed sensor in the presence of different explosives **a** for method–1 (1: TNT, 2: tetryl, 3: PA, 4: DNT, 5: HMX, 6: RDX, 7: PETN, 8: AN, 9: TATB at 500.0 mg L^{-1}–final conc.) and mixture solutions without using EDA–modified MNPs (10: DMSO+TNT, 11: DMSO+tetryl at 500.0 mg L^{-1}–in final conc.). **b** Color bleaching for method–2 (B: blank, 1: TNT, 2: tetryl, 3: PA, 4: DNT, 5: HMX, 6: RDX, 7: PETN, 8: AN, 9: TATB at 500.0 mg L^{-1}–final conc.)

method (512 nm for method–1 and 650 nm for method–2). It was necessary to see the additivity of absorbances (or absorbance differences) of these two nitro explosives when they were together. In order to investigate this situation, mixtures of 1:1 to 10:1 (*w*/*w*) TNT and tetryl were assayed using the proposed sensor. The A_{512} (method–1) and A_{650} (method–2) values of the resulting solutions were collected in Table 2, with mention of expected contribution from each component. The results in Table 2 show that precision in the analysis of binary (tetryl+TNT) mixtures increased as the ratio of TNT to tetryl was raised.

The results in Table 2 showed that precision in the analysis of binary (tetryl+TNT) mixtures increased as the ratio of TNT–to–tetryl was raised. The absorbance measurements for both TNT and tetryl (with respect to method–1) were made against a blank solution at 512 nm wavelength, with molar absorptivities of 7.17×10^3 for TNT and 2.06×10^4 for tetryl. This means that in binary (tetryl+TNT) mixtures, the tetryl constituent will initially produce a higher absorbance signal compared to that of TNT at the same level, and thus the precision for TNT will not be maximal at the start. However, as the ratio of TNT–to–tetryl in synthetic mixtures increases, TNT will constitute the increasingly greater percentage of the observed (overall) absorbance and the (constant) share contributed by tetryl will remain at a minor level. It is known that relative standard deviation gets lower as analyte concentration gets higher. It was reported that coefficient of variation or relative standard deviation, RSD, among inter-laboratory measurements

Table 2 Additivity of absorbances (or absorbance differences) of TNT and tetryl with respect to the proposed sensor in synthetic mixture solutions

Initial concentration of mixture solution	Mixing ratio (*w*/*w*)	Absorbance (% of excepted value)	
		Method–1	Method–2
4.0 mg L^{-1} Tetryl + 4.0 mg L^{-1} TNT	1:1	0.193 (86.16%)	1.051 (82.50%)
4.0 mg L^{-1} Tetryl	-	0.152	1.074
4.0 mg L^{-1} TNT	-	0.072	1.054
4.0 mg L^{-1} Tetryl + 8.0 mg L^{-1} TNT	1:2	0.281 (92.43%)	0.983 (90.17%)
4.0 mg L^{-1} Tetryl	-	0.152	1.074
8.0 mg L^{-1} TNT	-	0.152	0.982
4.0 mg L^{-1} Tetryl + 12.0 mg L^{-1} TNT	1:3	0.356 (86.20%)	0.942 (102.15%)
4.0 mg L^{-1} Tetryl	-	0.152	1.074
12.0 mg L^{-1} TNT	-	0.261	0.955
4.0 mg L^{-1} Tetryl + 16.0 mg L^{-1} TNT	1:4	0.438 (92.41%)	0.932 (92.12%)
4.0 mg L^{-1} Tetryl	-	0.152	1.074
16.0 mg L^{-1} TNT	-	0.322	0.929
4.0 mg L^{-1} Tetryl + 20.0 mg L^{-1} TNT	1:5	0.527 (100.96%)	0.889 (101.03%)
4.0 mg L^{-1} Tetryl	-	0.152	1.074
20.0 mg L^{-1} TNT	-	0.370	0.901
4.0 mg L^{-1} Tetryl + 40.0 mg L^{-1} TNT	1:10	0.843 (100.24%)	0.838 (97.23%)
4.0 mg L^{-1} Tetryl	-	0.152	1.074
40.0 mg L^{-1} TNT	-	0.689	0.841

For a given mixture, the absorbance decrements of individual explosive solutions with respect to a blank having abs. = 1.084 were added to obtain the total expected abs. decrement. The experimental abs. decrement of the binary explosive mixture solution was divided by this expected value to obtain the percentage abs. difference

increases for lower values of concentration in an exponential manner [41]. This is why precision for TNT increased with increasing ratios of TNT–to–tetryl in mixtures.

For both methods, the possible interferences of the explosives such as HMX, RDX, composite B, synthetic composite B, and composite C–4 to the detection of TNT were investigated. The TNT recovery (%) values in the presence of explosive substances (RDX, HMX, composite B, synthetic composite B, and composite C–4) are summarized in Table S1 to yield recoveries ranging between 91 and 107% (mostly close to 100%). The interference effect of 100–fold of concentration of humic acid was investigated in the presence of 20.0 mg L^{-1} initial concentration of TNT, and recovery of TNT was 99.00%.

The interfering effects of 100–fold concentration of common soil ions (Cl^-, NO_3^-, SO_4^{2-}, K^+, Mg^{2+}, Ca^{2+}, Cu^{2+}, Al^{3+}) and of camouflage materials (sugar, sweetener, acetylsalicylic acid, paracetamol–caffeine–based painkiller, and detergent) were investigated in the determination of TNT, and the obtained results are shown in Fig. 5 to yield near–quantitative recoveries.

Recovery of TNT and/or tetryl from real soil samples

Each sandy soil sample was polluted with TNT, tetryl, and tetrytol, separately. The polluted soil samples were extracted with acetone to transfer TNT, tetryl, and tetrytol from the soil to the extract phase. When the developed sensing methods–1 and 2 were applied to the extracts, TNT, tetryl, and tetrytol recoveries from sandy soil were 100.30, 97.20, and 97.00% for method–1, and 103.00, 94.30, and 98.60% for method–2, respectively.

Validation of the proposed method against GC–MS and LC–MS/MS

The solutions of 3.0–11.0 mg L^{-1} TNT and 1.0–15.0 mg L^{-1} tetryl in acetonitrile were analyzed with the GC–MS literature method [41] to generate the calibration equations, where the mean value of three consecutive repetitive injections was used for each calculation. The calibration equations between peak area and concentration were:

$$\text{Peak Area} = 3.64 \times 10^5\, C_{TNT} - 6.19 \times 10^5 \ (r = 0.9996) \text{ for TNT}$$

$$\left(C_{TNT} : \text{final concentration of TNT in mg } L^{-1}\right)$$

$$\text{Peak Area} = 2.50 \times 10^4\, C_{Tetryl} - 1.9 \times 10^4 \ (r = 0.9993) \text{ for tetryl}$$

$$\left(C_{Tetryl} : \text{final concentration of tetryl in mg } L^{-1}\right)$$

The solutions of 50.0–400.0 μg L^{-1} TNT and 50.0–400.0 μg L^{-1} tetryl in acetonitrile were analyzed with the LC–MS/MS literature method [38] to generate the calibration equations, where the mean value of three consecutive repetitive injections was used for each calculation. The calibration equations between peak area and concentration were:

$$\text{Peak Area} = 2.75\, C_{TNT} + 204.26 \ (r = 0.9979) \text{ for TNT}$$

$$\left(C_{TNT} : \text{final concentration of TNT in } \mu g\, L^{-1}\right)$$

Statistical comparison between the results of the proposed methods–1 and 2 and reference GC–MS and LC–MS/MS procedures applied to 5.0 mg L^{-1} TNT and 4.0 mg L^{-1} tetryl in acetonitrile was made on $N = 5$ repetitive analyses, essentially showing no significant difference in precision and accuracy between the results. The contaminated clay soil samples

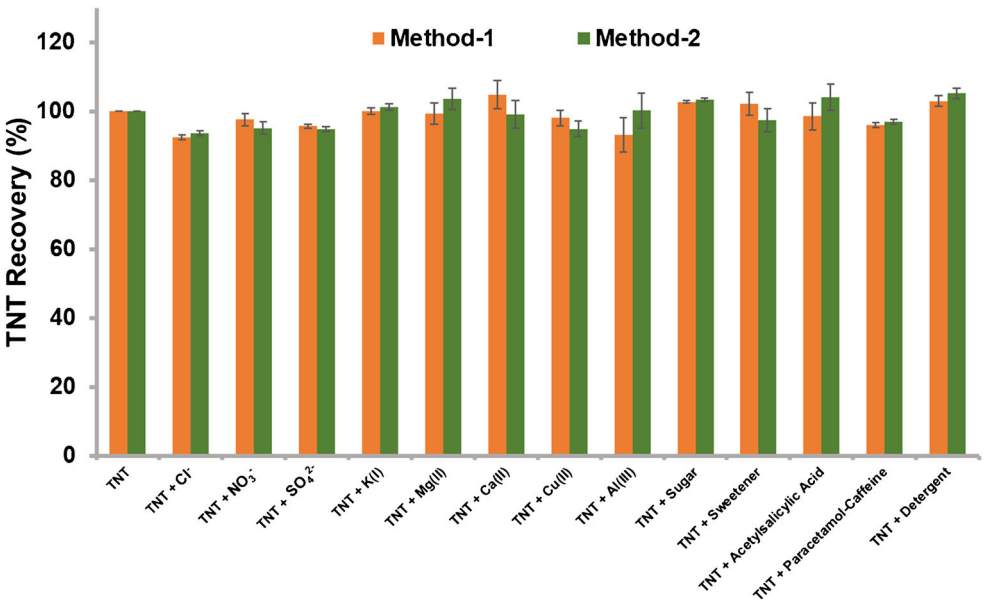

Fig. 5 Recovery of TNT at the initial concentration of 20.0 mg L^{-1} in the presence of common soil ions (Cl^-, NO_3^-, SO_4^{2-}, K^+, Mg^{2+}, Ca^{2+}, Cu^{2+}, and Al^{3+}) and camouflage materials (sugar, sweetener, acetylsalicylic, paracetamol–caffeine–based painkiller, and detergent) (orange bar; method–1, green bar; method–2)

were analyzed by LC–MS/MS in 1:100 (*v*/*v*) AcCN-diluted solution. Thus, the proposed method–1 and 2 procedures were validated against the GC–MS and LC–MS/MS method; the *t*- and *F*- tests were used for comparing the population means and variances, respectively. The confidence levels used in validation of findings were 95% (nominal 0.05 significance level) for both of *t*- and *F*- tests. Statistical parameters of the developed method and the reference GC–MS method were summarized in Table S2.

Conclusions

In this study, EDA–modified MNPs were synthesized with the polyol technique in one pot reaction. This is the first study involving the design of a unique reusable, selective, low–cost diamine–modified MNPs–based colorimetric sensor using the principle of charge–transfer complex formation for colorimetric detection of TNT/tetryl *via* two different methods combined in the same sensor. While the first of these methods is based on the direct (donor–acceptor) interaction of TNT and tetryl with EDA–modified MNPs, the other method is based on the nanozyme ability of EDA–modified MNPs to catalyze H_2O_2 oxidation to produce a blue–colored CT–complex from oxidized TMB, where TNT and tetryl in the medium caused bleaching of this color by inhibiting the catalytic ability of nanoparticles through a charge–transfer interaction. Our combination of charge−transfer and the nanozyme ability of EDA–functionalized Fe_3O_4 nanoparticles is expected to bring a new approach to dual function colorimetric sensor design for the sensitive determination of electron–withdrawing nitro explosive compounds. The sensitivities of the methods were sufficient to analyze soil samples in nitro explosive remediation sites with respect to the US EPA decontamination limits. When TNT and tetryl were together, they gave additive absorbances (or absorbance differences) using the two methods. Highly sensitive nanosensors can only be based on aggregation/disaggregation of nanoparticles which may be adversely affected by various physicochemical processes. However, a gain in sensitivity with aggregation/disaggregation is often accompanied by a loss in selectivity, as aggregation of nanoparticles may be often induced by various (mostly uncontrollable) physicochemical interactions including solvent and salt effects. In this work, the designed sensor is very stable, selective, and reusable along with its reasonable sensitivity. It is novel based on its contribution of unifying a double function in one single nanosensor. This is the first dual–function colorimetric sensor for TNT and tetryl using the same nanoparticles as sensing elements in two different detection systems involving either formation or bleaching of colored species.

Supplementary Information The online version contains supplementary material available at https://doi.org/10.1007/s00604-021-04877-z.

Acknowledgments The authors wish to express their gratitude to the Ministry of National Defence, Office of Technical Services, and to the Mechanical & Chemical Industry Corporation (MKEK) of Turkey for the donation of nitro and composite explosive samples. The authors extend their thanks to Istanbul University-Cerrahpaşa Research Fund (IUC BAP Unit) for the support given to Ph.D. Thesis Project–33833.

Declarations

Conflict of interest The authors declare no competing interests.

References

1. Fuller ME, Hatzinger PB, Rungmakol D, Schuster RL, Steffan RJ (2004) Enhancing the attenuation of explosives in surface soils at military facilities: combined sorption and biodegradation. Environ Toxicol Chem 23:313–324. https://doi.org/10.1897/03-187
2. Lewis TA, Newcombe DA, Crawford RL (2004) Bioremediation of soils contaminated with explosives. J Environ Manag 70:291–307. https://doi.org/10.1016/j.jenvman.2003.12.005
3. Adams VH (2015) Wildlife toxicity Assesment for N-methyl-N-2, 4,6-Tetranitroanaline (tetryl). In: Williams MA, Reddy G, Quinn MJ Jr, Johnson MS (eds) Wildlife toxicity assessments for chemicals of military concern, first edn. Elsevier, UK, Oxford, pp 205–216
4. Boopathy R (2005) Bioremediation of tetryl-contaminated soil using sequencing batch soil slurry reactor. Int Biodeterior Biodegradation 55:293–297. https://doi.org/10.1016/j.ibiod.2005.03.006
5. Akhgari F, Fattahi H, Oskei YM (2015) Recent advances in nanomaterial-based sensors for detection of trace nitroaromatic explosives. Sensors Actuators B Chem 221:867–878. https://doi.org/10.1016/j.snb.2015.06.146
6. Özcan Ç, Üzer A, Durmazel S, Apak R (2019) Colorimetric sensing of nitroaromatic energetic materials using surfactant-stabilized and dithiocarbamate-functionalized gold nanoparticles analytical letters 52:2794–2808. https://doi.org/10.1080/00032719.2019.1608555
7. Erçağ E, Üzer A, Apak A (2009) Selective spectrophotometric determination of TNT using a dicyclohexylamine-based colorimetric sensor. Talanta 78:772–780. https://doi.org/10.1016/j.talanta.2008.12.042
8. Puc U, Abina A, Rutar M, Zidanšek A, Jeglič A, Valušis G (2015) Terahertz spectroscopic identification of explosive and drug simulants concealed by various hiding techniques. Appl Opt 54:4495–4502. https://doi.org/10.1364/AO.54.004495
9. Kendziora CA, Furstenberg R, Papantonakis M, Nguyen V, McGill RA (2016) Broadband infrared imaging spectroscopy for standoff detection of trace explosives. International Society for Optics and Photonics 98362G:9836. https://doi.org/10.1117/12.2224049
10. Buryakov IA (2011) Detection of explosives by ion mobility spectrometry. J Anal Chem 66:674–694. https://doi.org/10.1134/S1061934811080077
11. Ewing AV, Kazarian SG (2017) Infrared spectroscopy and spectroscopic imaging in forensic science. Analyst 142:257–272. https://doi.org/10.1039/C6AN02244H
12. Lopez–Lopez M, Garcia–Ruiz C (2014) Infrared and Raman spectroscopy techniques applied to identification of explosives. TrAC

Trends Anal Chem 54:36–44. https://doi.org/10.1016/j.trac.2013.10.011
13. Sağlam S, Üzer A, Erçağ E, Apak A (2018) Electrochemical determination of TNT, DNT, RDX, and HMX with gold nanoparticles/poly(carbazole-aniline) film–modified glassy carbon sensor electrodes imprinted for molecular recognition of nitroaromatics and nitramines. Anal Chem 90:7364–7370. https://doi.org/10.1021/acs.analchem.8b00715
14. Sağlam Ş, Üzer A, Tekdemir Y, Erçağ E, Apak R (2018) Electrochemical sensor for nitroaromatic type energetic materials using gold nanoparticles/poly(o-phenylenediamine–aniline) film modified glassy carbon electrode. Talanta 139:181–188. https://doi.org/10.1016/j.talanta.2015.02.059
15. Kudr J, Haddad Y, Richtera L, Heger Z, Cernak M, Adam V, Zitka O (2017) Magnetic nanoparticles: from design and synthesis to real world applications. Nanomaterials 7:243. https://doi.org/10.3390/nano7090243
16. Beveridge JS, Stephens JR, Williams ME (2011) The use of magnetic nanoparticles in analytical chemistry. Annu Rev Anal Chem 4:251–273. https://doi.org/10.1146/annurev-anchem-061010-114041
17. Su L, Feng J, Zhou X, Ren C, Li H, Chen X (2012) Colorimetric detection of urine glucose based ZnFe2O4 magnetic nanoparticles. Anal Chem 84:5753–5758. https://doi.org/10.1021/ac300939z
18. Zhang H, Harpster MH, Park HJ, Johnson PA, Wilson WC (2010) Surface-enhanced Raman scattering detection of DNA derived from the West Nile virus genome using magnetic capture of Raman-active gold nanoparticles. Anal Chem 83:254–260. https://doi.org/10.1021/ac1023843
19. Shen YF, Tang J, Nie ZH, Wang YD, Ren Y, Zuo L (2009) Preparation and application of magnetic Fe_3O_4 nanoparticles for wastewater purification. Sep Purif Technol 68:312–319. https://doi.org/10.1016/j.seppur.2009.05.020
20. Faraji M, Yamini Y, Rezaee M (2010) Magnetic nanoparticles: synthesis, stabilization, functionalization, characterization, and applications. J Iran Chem Soc 7:1–37. https://doi.org/10.1007/BF03245856
21. Josephy PD, Eling T, Mason RP (1982) The horseradish peroxidase-catalyzed oxidation of 3,5,3′,5′-tetramethylbenzidine. Free radical and charge-transfer complex intermediates. J Biol Chem 257:3669–3675. https://doi.org/10.1016/S0021-9258(18)34832-4
22. Frey A, Meckelein B, Externest D, Schmidt MA (2000) A stable and highly sensitive 3,3′,5,5′-tetramethylbenzidine-based substrate reagent for enzyme-linked immunosorbent assays. J Immunol Methods 233:47–56. https://doi.org/10.1016/S0022-1759(99)00166-0
23. Gao L, Zhuang J, Nie L, Zhang J, Zhang Y, Gu N, Wang T, Feng J, Yang D, Perrett S, Yan X (2007) Intrinsic peroxidase-like activity of ferromagnetic nanoparticles. Nat Nanotechnol 2:577–583. https://doi.org/10.1038/nnano.2007.260
24. Can Z, Üzer A, Türkekul K, Erçağ E, Apak R (2015) Determination of triacetone triperoxide with a N,N-dimethyl-p-phenylenediamine sensor on Nafion using Fe_3O_4 magnetic nanoparticles. Anal Chem 87:9589–9594. https://doi.org/10.1021/acs.analchem.5b01775
25. Choodum A, Kanatharana P, Wongniramaikul W, Nic Daeid N (2013) Using the iPhone as a device for a rapid quantitative analysis of trinitrotoluene in soil. Talanta 115:143–149. https://doi.org/10.1016/j.talan”ta.2013.04.037
26. Sharma SP, Lahiri SC (2008) Absorption spectroscopic and FTIR studies on EDA complexes between TNT (2,4,6-trinitrotoluene) with amines in DMSO and determination of the vertical electron affinity of TNT. Spectrochim Acta MolBiomol 70:144–153. https://doi.org/10.1016/j.saa.2007.07.025
27. Xie C, Zhang Z, Wang D, Guan G, Gao D, Liu J (2006) Surface molecular self-assembly strategy for TNT imprinting of polymer nanowire/nanotube arrays. Anal Chem 78:8339–8346. https://doi.org/10.1021/ac0615044
28. Riskin M, Tel-Vered R, Bourenko T, Granot E, Willner I (2008) Imprinting of molecular recognition sites through electropolymerization of functionalized Au nanoparticles: development of an electrochemical TNT sensor based on π-donor−acceptor interactions. J Am Chem Soc 130:9726–9733. https://doi.org/10.1021/ja711278c
29. Jiang Y, Zhao H, Zhu N, Lin Y, Yu P, Mao L (2008) A simple assay for direct colorimetric visualization of trinitrotoluene at Picomolar levels using gold nanoparticles. Angew Chem Int Ed 47:8601–8604. https://doi.org/10.1002/ange.200804066
30. Tu R, Liu B, Wang Z, Gao D, Wang F, Fang Q, Zhang Z (2008) Amine-capped ZnS−Mn2+ nanocrystals for fluorescence detection of trace TNT explosive. Anal Chem 80:3458–3465. https://doi.org/10.1021/ac800060f
31. Qi W, Xu M, Pang L, Liu Z, Zhang W, Majeed S, Xu G (2014) Electrochemiluminescence detection of TNT by resonance energy transfer through the formation of a TNT–amine complex. Chem–Eur J 20:4829–4835. https://doi.org/10.1002/chem.201303710
32. Songvorawit N, Tuitemwong K, Tuitemwong P (2011) Single step synthesis of amino-functionalized magnetic nanoparticles with polyol technique at low temperature. ISRN Nanotechnology 2011:1–6. https://doi.org/10.5402/2011/483129
33. Sun M, Chen P, Zhao A, Zuo F (2019) Ultrasensitive detection of trinitrotoluene by Fe3O4@mTiO2/P-ATP-TNT/Au@Ag SERS sensor via synergetic effect. Anal Methods 11:1923–1929. https://doi.org/10.1039/C8AY02811G
34. Alizadeh T (2014) Preparation of magnetic TNT-imprinted polymer nanoparticles and their accumulation onto magnetic carbon paste electrode for TNT determination. Biosens Bioelectron 61:532–540. https://doi.org/10.1016/j.bios.2014.05.041
35. Zou WS, Wang YQ, Wang F, Sho Q, Zhang J, Liu J (2013) Selective fluorescence response and magnetic separation probe for 2,4,6-trinitrotoluene based on iron oxide magnetic nanoparticles. Anal Bioanal Chem 405:4905–4912. https://doi.org/10.1007/s00216-013-6873-6
36. USEPA (2014) Technical fact sheet–2,4,6-trinitrotoluene (TNT), Office of Solid Waste and Emergency Response, Washington, DC, USA, EPA-505-F-14-009
37. Sigman ME, Ma CY (2001) Detection limits for GC/MS analysis of organic explosives. Journal of Forensic Science 46:6–11. https://doi.org/10.1520/JFS14904J
38. Şen N, Üzek U, Aksoy Ç, Bora T, Atakol O (2015) Identification of organic explosives which have different structures by LC-MS-MS. SDU J Scien (E-Journal) 10:95–106
39. Ular N, Üzer A, Durmazel S, Erçağ E, Apak R (2018) Diaminocyclohexane-functionalized/Thioglycolic acid-modified gold nanoparticle-based colorimetric sensing of trinitrotoluene and tetryl. ACS Sens 3:2335–2342. https://doi.org/10.1021/acssensors.8b00709
40. Zhu W, Shen X, Zhu C, Li B, Hong J, Zhou X (2018) Turn-on fluorescent assay based on purification system via magnetic separation for highly sensitive probing of adenosin. Sensor Actuat B-Chem 259:855–861. https://doi.org/10.1016/j.snb.2017.12.147
41. Albert R, Horwitz W (1997) A heuristic derivation of the Horwitz curve. Anal Chem 69:789–790. https://doi.org/10.1021/ac9608376